

# Scenarios for the intentional release of Cs-137 from stacks of cement production factory: event analysis using the HotSpot code.

G. LATINI<sup>1</sup>, A. MALIZIA<sup>1</sup>, M. GELFUSA<sup>1</sup>, M. CARESTIA<sup>1</sup>, R. FIORITO<sup>2</sup>, F. D'AMICO<sup>1</sup>, A. GUCCIARDINO<sup>1</sup>, C. BELLECCI<sup>1</sup> and P. GAUDIO<sup>1</sup>

1. Dipartimento Ingegneria Industriale, Università degli Studi di Roma Tor Vergata, Via del Politecnico 1, 00133, Roma, ITALY

2. Dipartimento Medicina e Chirurgia, Facoltà di Medicina, Università degli Studi di Roma Tor Vergata, Via di Montpellier 1, 00133, Roma, ITALY

[Gaudio@ing.uniroma2.it](mailto:Gaudio@ing.uniroma2.it), [Malizia@ing.uniroma2.it](mailto:Malizia@ing.uniroma2.it)

*Abstract:* - There are several types of events that could result in dispersion of radioactive substances in the environment. These include both intentional and unintentional events. The extent of the contamination and impact on the environment and people depend greatly on the specific event and the radionuclide involved. In recent years, the concern for protection of urban populations against terrorist attacks involving radiological substances has attracted increasing attention. Models and computational codes have been developed and hypothetical scenarios have been formulated for establishing priority of countermeasures and protective actions; determining of generic operational guidelines; and assessment of risks for exposure population. The aim of the presents study is to illustrate the resultant effects of intentional release of Cs-137 from stacks of cement production industry. This is done through simulation of different scenarios using a computer code named HotSpot. The Total Effective Dose Equivalent (TEDE), which includes external and internal contributions for the whole absorbed dose, has been calculated for various atmospheric stability Pasquill categories [1]. The meteorological data on atmospheric stability conditions are setting as "mean wind speed" and the results have been analyzed and are presented here. The results indicate that atmospheric dispersion of a relatively small amount of Cs-137 has the potential to contaminate a relatively large area with the extent of contamination (area and activity) firstly dependent on Cs-137 particle size, the height of release, and local weather conditions.

*Key-Words:*- Dispersion Models, Radionuclides, Atmospheric Release, Cesium 137, HotSpot code

## 1 Introduction

Cesium is a soft, shiny, gold-colored metal. It reacts rapidly with oxygen or water. Its melting point is 301.55°K (28.4°C or 83.1°F) and boiling point is 951.6°K (678.5°C or 1253.2°F). Cesium-133 is the only naturally occurring isotope and is non-radioactive; all other isotopes, including cesium-137, are produced by human activity. Among these other isotopes, cesium-137 is the most common and was discovered by Glenn T. Seaborg and Margaret Melhase in the 1930s (Chase, 1967). The energy of its gamma ray is moderately high (662 keV) and depending on the source activity, the external dose irradiation of the body can be high. Cs is quite chemically reactive; its salts are very soluble in water and, consequently have a high environmental mobility, spreading quickly through the environment. Moreover, Cs-137 can be completely

absorbed by vital human organs such as lung, gastrointestinal tract and into wounds. Cesium behavior is analogous to the behavior of potassium. Once absorbed, cesium is quite uniformly distributed within the body, with the highest concentration in muscle tissues and the lowest in bones. Radiation exposure can occur both externally and internally. The toxicity of a given radioactive material and the associated doses for internal organs depend on some factors as: 1) type and energy of the radiation emitted by radionuclides, 2) the route of entry into the body, and 3) the chemical characteristics of the element, that determines the retention and distribution in the body.

Incidents involving commercial radioactive sources that have fallen out of control and entered into the public domain have been reported over the years. In some cases, sources entering into scrap processing

facilities have contaminated steel mills, resulting in millions of dollars in cleanup costs. In other cases, sources have been breached, exposing the public to harmful radiation. A classical example of a strong 'orphaned' source that suddenly appeared completely out of context in an inhabited area, causing severe health problems, is the Goiânia case in Brazil [2]. Here a 50.9 TBq  $^{137}\text{CsCl}$  source (in readily soluble powder form) caused contamination of a considerable area and many people, of which four were reported to have died within a weeks. The Goiânia experience is particularly interesting in relation to 'dirty bomb' scenarios, as this accident led to the contamination of a city area of a size equivalent to what might be affected by the contamination from a successful 'dirty bomb' attack. Although a multitude of transportation and migration pathways contributed to the spreading of the contamination, it has been reported that the primary cause of contamination of housing in the area was atmospheric dispersion. The Goiânia accident resulted in extensive panic, social disruption, great efforts and expenses for personal monitoring, decontamination of humans and area clean-up, for instance of roof tiles with Cs-137 contamination levels ranging up to some 700 kBq  $\text{m}^{-2}$ . In the wake of the terrorist attack on September 11th, 2001, there is a further security concern over radioactive materials. Traditionally, most commercial radioactive materials are managed less stringently than uranium or plutonium, since these commercial radioactive materials cannot be sources of nuclear weapons. However, the event raised the concern that such commercial radioactive materials could be cause of social disorder through their use in terrorist weapons, such as dirty bombs. The U.S. government and the International Atomic Energy Agency (IAEA) had shown their interest in a more stringent management system for commercial radioisotope materials and their plans were accelerated by the incident. Among these commercial radioactive materials, Cs-137 is one of those most dangerous because it is generating of beta and gamma emissions (gamma emission through its transitional daughter isotope barium-137m), large amount of radioactivity, and relatively long half-life.

Significant amounts of non-fissile radioactive materials are stored in medical centers to diagnose and treat illnesses, research laboratories, processing plants to irradiate food to eliminate microbes, radiothermal generators, and oil well surveying instruments. Although those facilities lack the types or volumes of materials suitable for producing nuclear weapons, they contain large amounts of

radioactive material such as cesium-137, cobalt-60, strontium-90, and iridium-192. The possibility of terrorists using conventional explosives coupled with those non-fissile radioactive materials to create a radiological dispersion device commonly called a 'dirty bomb' has transformed concerns about illicit commercial radioactive materials relatively obscure topic into a major international security.

A radiological attack would not produce the mass casualties due to the blast and significant radiation exposure associated with a nuclear event, but it nonetheless could result in radiation concentrations exceeding International Commission on Radiological Protection (ICRP) guidelines for limiting exposures to gamma radiation. Such an incident could create a variety of impacts ranging from extensive contamination requiring remediation, to panic and economic disruption, to long-term exposure of civilian populations to low levels of radiation exceeding natural background levels. The actual impact of terrorists releasing non-weapons grade materials is contingent upon a variety of factors including the specific isotope used, the amount of material released, the aerosol properties of the particles released, local-scale meteorological conditions within a distance  $\leq 10$  km from the initial release point (i.e., wind speed, wind direction, other key meteorological parameters), local-scale topography (i.e. location and size of buildings), and the type of device used to release the material (i.e., conventional explosive).

For these reasons, the studies and developments of techniques and methods of atmospheric dispersion modeling of radioactive material in radiological risk assessment and emergency response over the past 50-60 years are evolved. The three marked types of dispersion models, which may describe the development of dispersion modeling techniques for the application in radiological risk assessments and emergency responses, are Gaussian plume models in the 1960s and 1970s, Lagrangian – puff models and particle random walk models in the 1980s - 1990s, and CFD (Computational Fluid Dynamics) models in the 2000s [3, 5-19].

In this study, a potential scenario of radiological release is simulated using HotSpot, which is able to estimate the radiation dispersion in an area. The main purpose of this research is the evaluation of different scenarios for initial aerosol dispersion by stacks of a cement factory in function of different atmospheric stability scenarios.

## 2 Methods

### 2.1 Source term and accident scenario

We have assumed that the amount of Cs-137 involved in the accident scenario is  $1.11 \times 10^{14}$  Bq. This amount of cesium is chosen for modeling because it is comparable to the amounts typically available in commercial radioactive sources.

The release scenario considers the introduction of the radionuclide inside a limestone fragmentation line and subsequent transmission to the filtration system, as shown in Figure 1.

The production plant considered in this case study is composed of three stacks and their characteristics are summarized in Table 1.

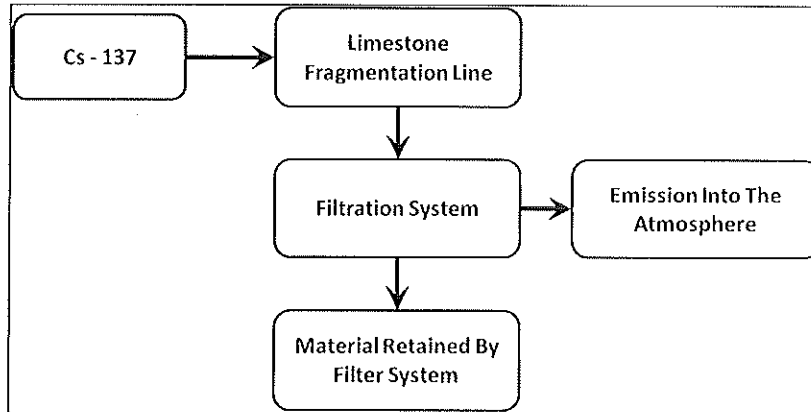


Fig. 1: Introduction of Radionuclide Inside the Cement Production Line

Table 1: Technical characteristics of stacks of cement production plant.

PROPERTY	STACK 1	STACK 2	STACK 3
Height Above Sea Level	180 m	180 m	180 m
Physical Stack Height	92 m	92 m	92 m
Stack Diameter	3.1 m	1.8 m	1.8 m
Air Temperature	22°C	22°C	22°C
Stack Effluent Temperature	80°C	95°C	110°C
Stack Exit Velocity	17.5 m/s	10.4 m/s	8.2 m/s
Flue Gas Flow	475000 Nm <sup>3</sup> /h	95000 Nm <sup>3</sup> /h	75000 Nm <sup>3</sup> /h

The raw material preparation stage of cement manufacture results in the production of a raw mix that is in a suitable state for feeding to the kiln in which it is converted by heat into clinker. From data obtained from the literature, it was possible to estimate the average hourly volume of raw material sent to the oven, needed for the production of cement. In this work we have assumed that during a typical production day, the raw materials sent to the production facilities were about 208 t/h, corresponding to  $208 \times 10^3$  kg/h, which is equivalent to  $4.99 \times 10^6$  kg/day. In this scenario, assuming that

the filtration system works properly, the percentage of dust emitted into the atmosphere respect to the volume introduced into the system, is about 0.0033%.

In this case study, the source of Cs-137 was introduced through limestone fragmentation line, and radionuclide will be subject to the same filtration process of raw materials with emissions in atmosphere of 0.0033% the initial amount. This estimation is conservative because we have assumed that Cs-137 is not all trapped in the clinker matrix. All the remaining radiogenic material will be

retained by filters and/or reintroduced to cycle until find it in the final product (clinker – cement). In order to analyze the release scenario a "virtual stack" has been defined, obtained by normalizing respect to the total flow rate the characteristic parameters of each stack, according to the following calculation scheme:

$$Q_T = Q_1 + Q_2 + Q_3 = 645.000 \text{ Nm}^3/\text{h} \quad (1)$$

$$d = d_1 \frac{Q_1}{Q_T} + d_2 \frac{Q_2}{Q_T} + d_3 \frac{Q_3}{Q_T} = 2,8 \text{ m} \quad (2)$$

$$v = v_1 \frac{Q_1}{Q_T} + v_2 \frac{Q_2}{Q_T} + v_3 \frac{Q_3}{Q_T} = 15,4 \text{ m/s} \quad (3)$$

$$T = T_1 \frac{Q_1}{Q_T} + T_2 \frac{Q_2}{Q_T} + T_3 \frac{Q_3}{Q_T} = 86^\circ\text{C} \quad (4)$$

Where:

$Q_T$  = Total gas flow rate.

$Q_1, Q_2, Q_3$  = Gas flow rate of single stack.

$d$  = Stack diameter of virtual stack.

$d_1, d_2, d_3$  = Stack diameter of single stack.

$v$  = Exit velocity of virtual stack.

$v_1, v_2, v_3$  = Exit velocity of single stack.

$T$  = Effluent temperature of virtual stack.

$T_1, T_2, T_3$  = Effluent temperature of single stack.

Table 2: summarize the characteristic parameters of "virtual stack".

**Table 2:** Parameters of "virtual stack"

Height Above Sea Level	180 m
Physical Stack Height	92 m
Stack Diameter	2.8 m
Air Temperature	22°C
Stack Effluent Temperature	86°C
Stack Exit Velocity	15.4 m/s
Flue Gas Flow	645000 Nm <sup>3</sup> /h

## 2.2. Meteorological conditions and atmospheric stability classes used in HotSpot

Meteorologists distinguish several states of the local atmosphere: A, B, C, D, E, F. These states can be tabulated as a function of weather conditions, wind speed and time of day. According to the stability category the attack can result in a wide spectrum of lethal effects. Therefore the potential terrorist will certainly take that into account, just as it happens by war-planners, so that the lethal effects are maximized. The stability of the atmosphere depends on the temperature difference between an air parcel and the air surrounding it. Therefore, different levels

of stability can occur based on how large or small the temperature difference is between the air Parcel and the surrounding air. [20-24]

The stability classes used for this work are referred to Pasquill – Gifford stability classes and are depicted in Table 3. As can be seen in the Table, stabilities A, B, and C refer to daytime hours with unstable conditions. Stability D is representative of overcast days or nights with neutral conditions. Stabilities E and F refer to nighttime, stable conditions and are based on the amount of cloud cover. Thus, classification A represents conditions of the greatest instability, and classification F reflects conditions of the greatest stability. For all stability class the wind direction was set at 270 degrees respect north direction, . The value of wind speed assumed for the simulation are summarize in Table 3.

**Table 1:** Pasquill – Gifford stability classes and ground wind speed. [1]

Ground wind speed (m/s)	Sun high in sky	Sun low in sky or cloudy	Night time
1	A	B	F
2.5	A	C	E
3.5	B	C	D
5	C	D	D
7.5	C	D	D

## 2.3. Radiation dose calculations

All calculations have been performed using HotSpot Version 2.07.1 running on a PC computer [25-28]. The "standard area terrain" type has been used to take into account the conservative condition because in this case the characteristic of roughness lengths is in the range of 0.01 – 0.1 meters. The deposition velocity of the particles is assumed to be 20 cm/s, whereas a value of 40 cm/s is used for the inhalable fraction.

The breathing rate of exposed person is based on the standard rates established by HotSpot code and taken from the International Commission on Radiological Protection (ICRP) for reference man. The standard rate of  $3.33 \times 10^{-4}$  m<sup>3</sup>/sec, equivalent to 1.2 m<sup>3</sup>/hr: this value corresponding to light activity and is recommended for doses received as a result of an accident. The height of the receptors is set to be 1.5 m.

Source term values used to establish the outline dose of TEDE and Ground Surface Deposition contour plot are shown in Table 4.

**Table 4:** Source term value used in HotSpot simulation

	TEDE (Sv)	GROUND SURFACE DEPOSITION (kBq/m <sup>2</sup> )
Inner Contour Dose	$1.00 \times 10^{-6}$	1
Middle Contour Dose	$1.00 \times 10^{-7}$	0.1
Outer Contour Dose	$1.00 \times 10^{-8}$	0.01

To evaluate the dose conversion factors HOTSPOT uses the publication FGR 11 for all calculations. For the purpose of this work, the sample time has been set to 60 minutes and the holdup time is assumed 0 minutes, to simulate that the material is immediately released into the atmosphere.

All simulation scenarios have been performed including plume passage inhalation and submersion, ground shine (without the weathering correction factor) and re-suspension (with re-suspension factor obtained from [4])

### 3. Results

For realistic and reliable estimation of contamination (total dose, ground deposition etc.), following a typical dispersion of radiological materials into the atmosphere, then it is necessary to know the cloud properties:

- dimensions (volume, effective height);
- particles size distribution within the cloud;

and all the functions of the source term amount, space and time, wind speed and atmospheric stability class.

In this section the graphic results obtained for any scenario considered are reported. For each class of stability and wind speed value the diagrams TEDE and Ground Deposition diagrams have been plotted as function of downwind distance.

The doses calculated could be received by a person at height of 1.5 m from ground level who remained within the plume for the entire duration of the cloud passage. As the release occurs at 92 m stack height, the doses first increase with distance, reach a maximum value and then decrease.

The heat and smoke of the explosion will lift small particles of Cesium up into the air and, according to the nature of the released radioactive material, these particles will settle to the ground as they are carried along by the wind contaminating the ground surface. Large particles will contaminate the immediate vicinity of the explosion while smaller (fine and mostly inhalable) ones will travel large distances or will rise up at high altitudes until they are deposited on the ground. Obviously, non-inhalable material will have a much larger deposition velocity than inhalable ones.

Table 1 summarizes some physical parameters obtained from the Hotspot simulations.

Setting the wind speed and the geometry of the stack, the change of atmospheric stability class affects the distance at which the maximum dose occurs, the TEDE variation and the effective height of release.

In Figure 1 the diagram of the Total Effective Dose Equivalent as a function of downwind distance is shown. The location of the maximum dose gives the plume touchdown distance. For all Scenario considered, it can be observed that the plume touchdown distance (point of maximum dose) increases with increasing of the stability; however the maximum dose value reduces with increasing of the stability. Only for Scenario 1, for the Pasquill stability class F, the inner dose did not exceed. On the other hand, the worst case represented by the case Scenario 2 for the stability class A.

Table 2: Main parameters obtained for HotSpot code

<b>SCENARIO 1</b>			
	<b>Stability Class A</b>	<b>Stability Class B</b>	<b>Stability Class F</b>
<b>Effective Release Height</b>	432 m	432 m	149 m
<b>Maximum Dose Distance</b>	1.4 km	2.2 Km	23 Km
<b>Maximum TEDE</b>	$6.25 \times 10^{-6}$ Sv	$4.16 \times 10^{-6}$ Sv	$1.08 \times 10^{-7}$ Sv
<b>Exceeds inner dose out to</b>	4.5 Km	5.5 Km	Not Exceeded
<b>Exceeds middle dose out to:</b>	12.5 Km	13.6 Km	30 Km
<b>Exceeds outer dose out to</b>	34.6 Km	32.9 Km	74 Km
<b>SCENARIO 2</b>			
	<b>Stability Class A</b>	<b>Stability Class C</b>	<b>Stability Class E</b>
<b>Effective Release Height</b>	234 m	222 m	152 m
<b>Maximum Dose Distance</b>	0.82 km	2.2 Km	8.1 Km
<b>Maximum TEDE</b>	$1.18 \times 10^{-5}$ Sv	$7 \times 81 \times 10^{-6}$ Sv	$1.39 \times 10^{-6}$ Sv
<b>Exceeds inner dose out to</b>	4.12 Km	8.9 Km	12.5 Km
<b>Exceeds middle dose out to:</b>	13.05 Km	23.2 Km	36 Km
<b>Exceeds outer dose out to</b>	43.51 Km	51 Km	58.10 Km
<b>SCENARIO 3</b>			
	<b>Stability Class B</b>	<b>Stability Class C</b>	<b>Stability Class D</b>
<b>Effective Release Height</b>	195 m	186 m	174 m
<b>Maximum Dose Distance</b>	1.1 Km	1.8 Km	4.4 Km
<b>Maximum TEDE</b>	$1.05 \times 10^{-5}$ Sv	$8.52 \times 10^{-6}$ Sv	$3.11 \times 10^{-6}$ Sv
<b>Exceeds inner dose out to</b>	5.3 Km	8.6 Km	12.9 Km
<b>Exceeds middle dose out to:</b>	16.7 Km	25.9 Km	30.7 Km
<b>Exceeds outer dose out to</b>	55.8 Km	64.1 Km	49 Km
<b>SCENARIO 4</b>			
	<b>Stability Class C</b>	<b>Stability Class D</b>	
<b>Effective Release Height</b>	159 m	151 m	
<b>Maximum Dose Distance</b>	1.5 Km	3.5 Km	
<b>Maximum TEDE</b>	$8.54 \times 10^{-6}$ Sv	$3.5 \times 10^{-6}$ Sv	
<b>Exceeds inner dose out to</b>	7.8 Km	12.4 Km	
<b>Exceeds middle dose out to:</b>	26.7 Km	32.6 Km	
<b>Exceeds outer dose out to</b>	78.3 Km	58.6 Km	
<b>SCENARIO 5</b>			
	<b>Stability Class C</b>	<b>Stability Class D</b>	
<b>Effective Release Height</b>	137 m	132 m	
<b>Maximum Dose Distance</b>	1.3 Km	3 Km	
<b>Maximum TEDE</b>	$8.07 \times 10^{-6}$ Sv	$3.65 \times 10^{-6}$ Sv	
<b>Exceeds inner dose out to</b>	6.8 Km	11.7 Km	
<b>Exceeds middle dose out to</b>	26.5 Km	35 Km	
<b>Exceeds outer dose out to</b>	93.6 Km	73.7 Km	

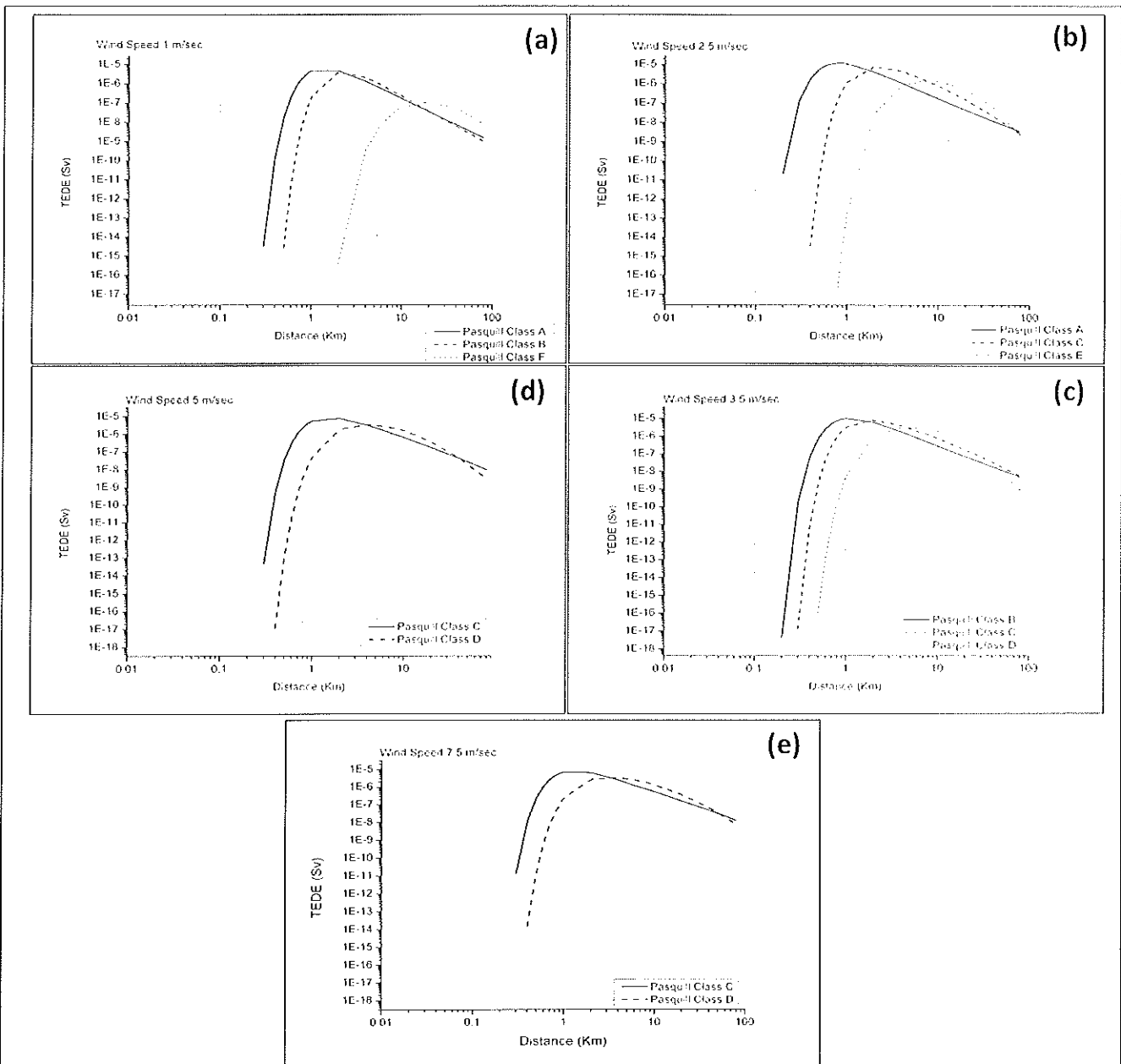


**Fig. 2:** Total Effective Dose Equivalent as a function of downwind distance: (a): Scenario 1; (b) Scenario 2; (c) Scenario 3; (d) Scenario 4; (e) Scenario 5

In case of radiological release the estimation of the area contaminated is a very important point in order to manage the operation needed to decontaminate, the impact on the environment and population and the cost of the decontamination. Experience shows that a radiological incident could contaminate a large area and that cleanup would be expensive. The reality is more complex: area and cost depend on the maximum acceptable dose and other assumptions chosen for a scenario. Furthermore, atmospheric processes can be reduced or enhance dispersion and deposition after the initial release of radiological

source. Three of the most important parameters that drive the phenomena are wind speed, atmospheric stability, and precipitation. Dilution occurs most rapidly at high wind speeds, with unstable atmospheric condition with sharp temperature gradients in which the surface layer is hotter than the air above it, and during precipitation. For these reasons, in this case study The Ground Surface Deposition as function of downwind distance has been evaluated. The Figure 3 shown the diagram for each Scenario considered.

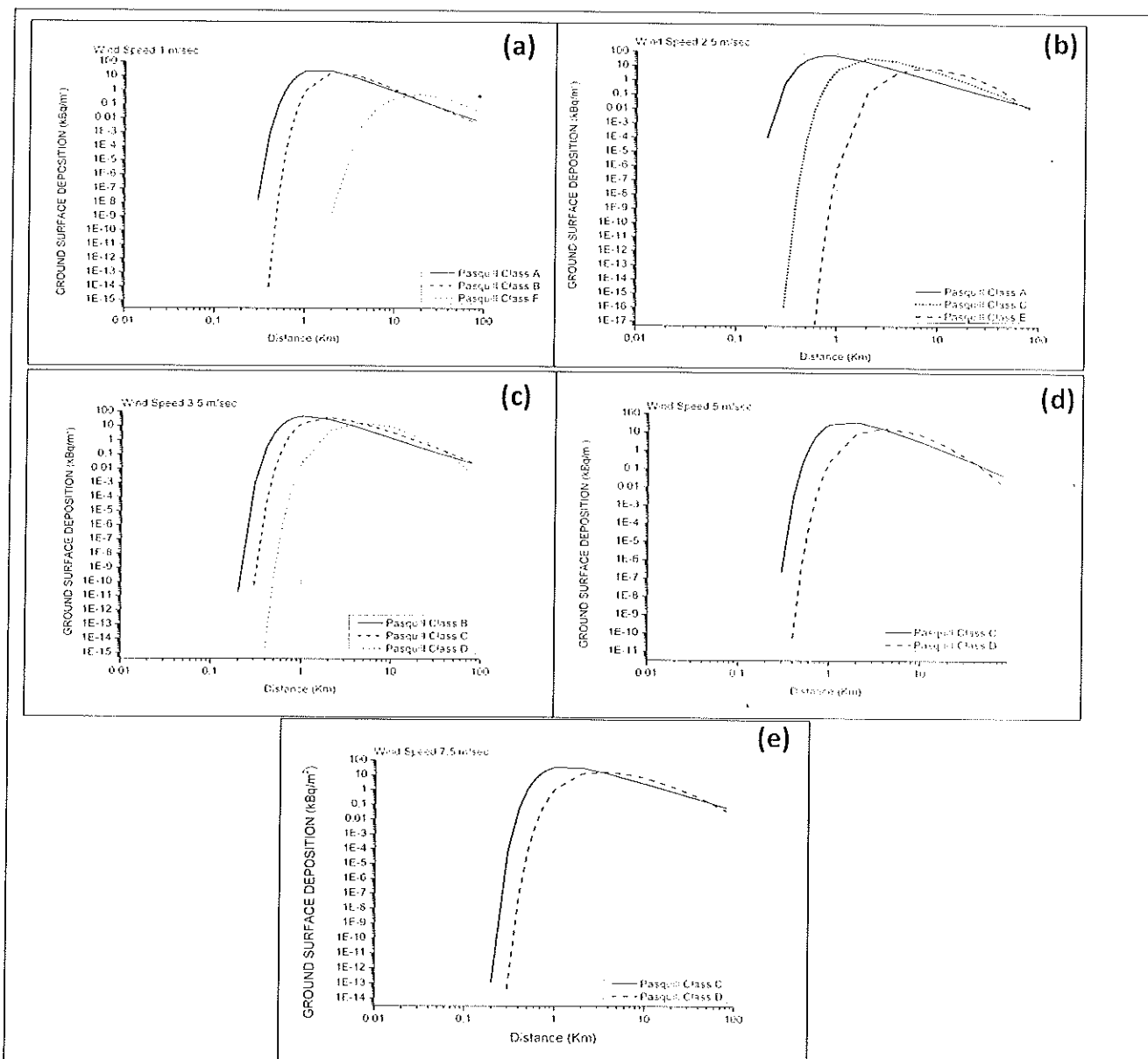


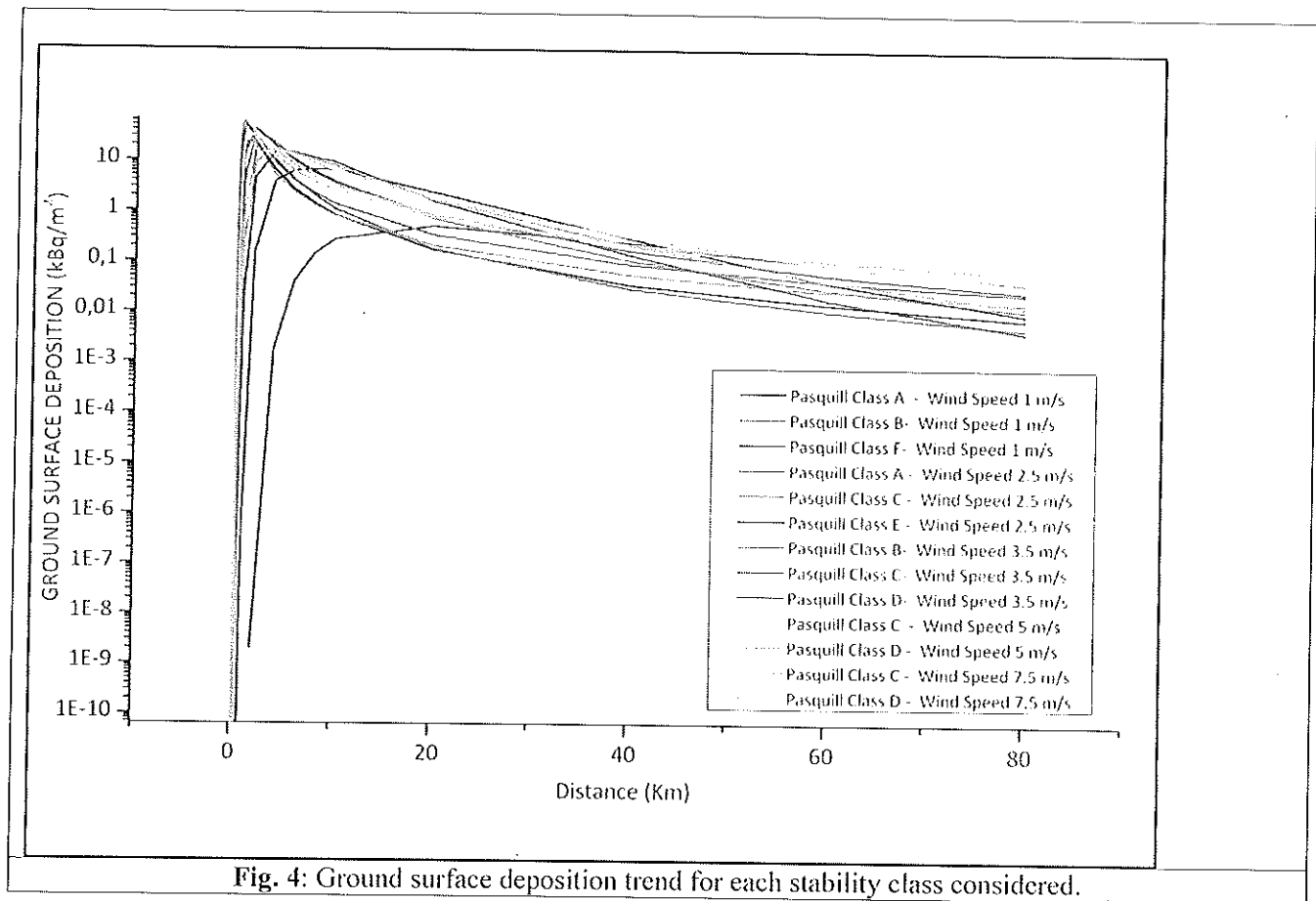
**Fig. 3:** Ground Surface Deposition as a function of distance downwind: a): Scenario 1; (b) Scenario 2; (c) Scenario 3; (d) Scenario 4; (e) Scenario 5.

There are several relationships between ground-level concentrations and concentrations at the level of the plume release point in function of meteorological conditions. For elevated concentration material, the maximum concentrations for time periods of about half an hour can occur with fumigation conditions when an unstable layer increases vertically to mix downward a plume previously discharged within a stable layer. With small different height ( $\Delta H$ ), the fumigation can occur close to the source but will be of relatively short duration. For large  $\Delta H$ , the fumigation will occur some distance from the stack (perhaps 30 to 40 km), but can persist for a longer time interval.

Concentrations considerably lower than those associated with fumigations, but of significance, can occur with neutral or unstable conditions when the dispersion upward is severely limited by the existence of a more stable layer above the plume, for example, an inversion. Under stable conditions the maximum concentration at ground-level from big amount of material are less than those occurring under unstable conditions and occur at greater distances from the source. Because the maximum occurs at greater distances, concentrations that are below the maximum but still significant can occur over large areas. This becomes increasingly significant if the emissions are from more than one



source. Figure 4 summarizes the trends of curves for each stability class considered.



#### 4. Conclusions

Different scenarios of radiological release in atmosphere function of a Pasquill class and wind speed were analyzed, and the plume extension in conjunction with the ground surface deposition of each scenario were evaluated. The data used to create the parameters include: type of radioactive material, stack geometry and dimension, effluent parameters and meteorological conditions. The radioactive material for evaluation was selected based on information such as frequently used material in usual and activity values characterizing medical and industrial applications .

The results indicate a relatively small amount of Cs-137 has the potential to contaminate a relatively large area with the extent of contamination dependent on Cs-137 particle size, the height of release, and local weather conditions.

Modeling the dispersion of radioactive aerosols throughout an urban landscape, especially with accurate knowledge of radionuclide, geometry of source and meteorology, is indispensable for

assessing the potential consequences of a terrorist incident and implementing effective emergency response, health services, and decontamination decisions

Considering that the atmospheric release of radioactive material might occur at high-density crowd events or in densely – populated urban areas, it is possible to envisage that thousands of people might be exposed to ionizing radiation. Additionally, operations in these contaminated areas might result in intervention teams receiving sufficient radiation doses that are of particular concern and should be managed. [29,30]

For first responders, given the dominance of the inhalation pathway, the modeling results underscore the importance of adequate respiratory protection to reduce the amount of radioactive material inhaled. And, prior to initiating follow-up evacuation and environmental remediation activities, the results also emphasize the importance of initial screening to delineate quickly TEDE “boundary lines” as a beginning point for determining the extent of the

“hot zone” for potential ground shine exposure created by accidental radiological release

In an operational situation it is important to obtain useful results as quickly as possible. HOTSPOOT is particularly good in this sense, as it takes only moments to input the scenario parameters, and results are calculated virtually instantaneously.

This application of computer modeling has implications for identifying the potential consequences of a intentional or non intentional radiological releases.

The consequence data obtained from this study can be used for the establishment of response measures against radiological terror. In order to enhance its effectiveness, more data for evaluation based on reliable scenarios is needed.

#### References:

- [1] R.R. Draxler, Determination of atmospheric diffusion parameters, *Atmospheric Environment*, Vol.10, No.2, 1976, pp. 99-105.
- [2] International Atomic Energy Agency, *The radiological Incident in Goiânia*, Pub. 815, Vienna 1988.
- [3] Y. Rentai, Atmospheric dispersion of radioactive material in radiological risk assessment and emergency response, *Progress in Nuclear Science and Technology*, Vol 1, 2011, pp. 7-13.
- [4] Report No.129 of National Council on Radiation Protection and Measurements, (1999) .
- [5] M Benedetti, P Gaudio, I Lupelli, Malizia A., M T Porfiri, M Richetta (in stampa). Large Eddy Simulation of Loss of Vacuum Accident in STARDUST facility. “Fusion engineering and design”, ISSN: 0920-3796
- [6] P Gaudio, Malizia A., I Lupelli (2011). RNG k-e modelling and mobilization experiments of loss of vacuum in small tanks for nuclear fusion safety applications. “International journal of systems applications, engineering & development”, vol. 5; p. 287-305, ISSN: 2074-1308
- [7] FED 2013
- [8] M.Benedetti, P.Gaudio, I.Lupelli, Malizia A., M.T.Porfiri, M.Richetta (2011). Influence of Temperature Fluctuations, Measured by Numerical Simulations, on Dust Resuspension Due to L.O.V.As . International journal of systems applications, engineering & development, vol. 5; p. 718-727, ISSN: 2074-1308
- [9] C Bellecci, P Gaudio, I Lupelli, Malizia A., M T Porfiri, R Quaranta, M Richetta (2011). Validation of a Loss of Vacuum Accident Computational Fluid Dynamics (CFD) model. *Fusion engineering and design*, vol. 86; p. 2774-2778, ISSN: 0920-3796
- [10] C Bellecci, P Gaudio, I Lupelli, Malizia A., M T Porfiri, R Quaranta, M Richetta (2011). STARDUST experimental campaign and numerical simulations: Influence of obstacles and temperature on dust resuspension in a Vacuum Vessel under LOVA. *Nuclear fusion*, vol. 51, ISSN: 0029-5515, doi: doi:10.1088/0029-5515/51/5/053017
- [11] C Bellecci, P Gaudio, I Lupelli, Malizia A., M T Porfiri, R Quaranta (2011). Loss of Vacuum Accident (LOVA): Comparison of Computational Fluid Dynamics (CFD) flow velocities against experimental data for the model validation. *Fusion engineering and design*, vol. 86; p. 330-340, ISSN: 0920-3796
- [12] M.Benedetti, P.Gaudio, I.Lupelli, Malizia A., M.T.Porfiri, M.Richetta (2011). Scaled Experiment for Loss of Vacuum Accidents in Nuclear Fusion Devices: Experimental Methodology for Fluid-Dynamics Analysis in STARDUST Facility. In: WSEAS - CSCC Multiconference Conference Proceedings. Corfu Island, Greece, July 14-16 2011, p. 142-148, ISBN/ISSN: 978-1-61804-020-6
- [13] T. Pinna, L.C. Cadwallader, G. Cambi, S. Ciattaglia, S. Knipe, F. Leuterer, Malizia A., P. Petersen, M.T. Porfiri, F. Sagot, S. Scales, J. Stober, J.C. Vallet, T. Yamanishi (2010). Operating experiences from existing fusion facilities in view of ITER safety and reliability. *Fusion engineering and design*, vol. 85; p. 1410-1415, ISSN: 0920-3796
- [14] C Bellecci, P Gaudio, I Lupelli, Malizia A., M T Porfiri, R Quaranta, M Richetta (2010). Validation of a Loss Of Vacuum Accident (LOVA) computational fluid dynamics (cfd) model. In: Proceedings 26th Symposium on Fusion Technology. Porto, Portugal, 27 September-1 October 2010
- [15] C. Bellecci, P. Gaudio, I.Lupelli, Malizia A., M.T.Porfiri, R. Quaranta, M.Richetta (2010). Experimental mapping of velocity flow field in case of L.O.V.A inside STARDUST facility. In: EPS Conference Proceedings 2010. Dublin-Ireland, 21-25 June 2010

- [16] P.Gaudio, Malizia A., I.Lupelli (2010). Experimental and Numerical Analysis of Dust Resuspension for Supporting Chemical and Radiological Risk Assessment in a Nuclear Fusion Device. In: Conference Proceedings - International Conference on Mathematical Models for Engineering Science (MMES' 10). Puerto De La Cruz, Tenerife, 30/11/2010 - 30/12/2010, p. 134-147, ISBN/ISSN: 978-960-474-252-3
- [17] C.Bellecci, P.Gaudio, I.Lupelli, Malizia A., M.T.Porfiri, R.Quaranta, M. Richetta (2009). Characterization of divertor influence in case of LOVA: Analysis stardust facility and thermofluidodynamics simulation. In: EPS2009 Proceedings. Sofia-Bulgaria, 29 June- 3 July 2009
- [18] C.Bellecci, P.Gaudio, I.Lupelli, Malizia A., M.T.Porfiri, R.Quaranta, M. Richetta (2009). Velocity flow field characterization inside STARDUST experimental facility: Comparison between experimental campaign and numerical simulation results. In: ICENES2009 Proceedings. Erice-Portugal, 29 June- 3 July 2009, ISBN/ISSN: 978-989-96542-1-1
- [19] C. Bellecci, P. Gaudio, I.Lupelli, Malizia A., M.T.Porfiri, M. Richetta (2008). Dust mobilization and transport measures in the STARDUST facility. In: EPS2008 Proceedings, 35th EPS Conference on Plasma Physics. Hersonissos - Crete - Greece, 9 - 13 June 2008, vol. ECA Vol.32, p. P-1.175
- [20] P. Gaudio, M. Gelfusa, I. Lupelli, Malizia A., A. Moretti, M. Richetta, C. Serafini (2012). Early forest fires detection using a portable CO<sub>2</sub> Dial system: preliminary results. In: Proceedings 14<sup>o</sup> Convegno Nazionale delle Tecnologie Fotoniche, Firenze, 15-17 maggio 2012 – ISBN . Firenze, Italia, Maggio 2012, ISBN/ISSN: 9788887237146.
- [21] P.Gaudio, M. Gelfusa, Malizia A., M. Richetta, C.Serafini, P. Ventura, C. Bellecci, L.De Leo, T.Lo Feudo, A. Murari (2012). A portable LIDAR system for the early detection: FfED system - a case study. In: Advances in Fluid Mechanics and Heat & Mass Transfer Conference Proceedings. Istanbul - Turkey, July 21-23, 2012, p. 208-214, ISBN/ISSN: 978-1-61804-114-2
- [22] P Gaudio, M Gelfusa, I Lupelli, Malizia A., A Moretti, M Richetta, C Serafini, C Bellecci (2011). First open field measurements with a portable CO<sub>2</sub> lidar/ dial system for early forest fires detection. In: SPIE Conference Proceedings, p. 818213-1-818213-7
- [23] C. Bellecci, P. Gaudio, M. Gelfusa, Malizia A., M. Richetta, C. Serafini, P. Ventura (2010). Planetary boundary layer (PBL) monitoring by means of two laser radar systems: experimental results and comparison. In: SPIE proceedings
- [24] C. Bellecci, P. Gaudio, M.Gelfusa, T. Lo Feudo, Malizia A., M. Richetta, P.Ventura (2009). Raman water vapour concentration measurements for reduction of false alarms in forest fire detection. In: SPIE2009 Proceedings. Berlin - Germany, 31 August - 3 September 2009
- [25] D&T Bull. De Angelis
- [26] Malizia A., R.Quaranta, R.Mugavero (2010). CBRN Events in the Subway System of Rome : Technical-Managerial Solutions for Risk Reduction. Defence S&T technical bulletin, vol. 33; p. 140-157, ISSN: 1985-6571
- [27] Malizia A., I Lupelli, F D'Amico, A Sassolini, A Fiduccia, A M Quarta, R Fiorito, A Gucciardino, M Richetta, C Bellecci, P Gaudio (2012). Comparison of Software for Rescue Operation Planning During an Accident in a Nuclear Power Plant. Defence s & t technical bulletin, vol. 5; p. 36-45, ISSN: 1985-6571
- [28] R Gallo, P De Angelis, N Gallo, Malizia A., A Fiduccia, F D'Amico, R Fiorito, A Gucciardino, M Richetta, C Bellecci, P Gaudio (2012). Development of a software for the identification mapping of radiological diffusion in order to improve the rescue operations. In: MIMOS Conference Proceedings. Roma, 9-11 Ottobre 2012
- [29] Malizia A., R.Quaranta, R.Mugavero, R.Carcano, G.Franceschi (2011). Proposal of the prototype RoSyD-CBRN, a robotic system for remote detection of CBRN agents. Defence S&T technical bulletin, vol. 4; p. 64-76, ISSN: 1985-6571
- [30] O Cenciarelli, Malizia A., M Marinelli, S Pietropaoli, R Gallo, F D'Amico, C Bellecci, R

Fiorito, A Gucciardino, P Gaudio (in stampa).  
Evaluation of biohazard management of the italian  
national fire brigade . defence S&T technical  
bulletin, ISSN: 1985-657